scientific reports

OPEN

Superconductivity of thulium substituted clathrate hexahydrides at moderate pressure

Hongyu Huang[1], Chao Deng[1], Hao Song[1], Mingyang Du[1]✉, Defang Duan[2], Yanhui Liu[1] & Tian Cui[1,2]✉

Due to the BCS theory, hydrogen, the lightest element, would be the prospect of room-temperature superconductor after metallization, but because of the difficulty of the hydrogen metallization, the theory about hydrogen pre-compression was proposed that the hydrogen-rich compounds could be a great option for the high T_c superconductors. The superior properties of TmH_6, YbH_6 and LuH_6 indicated the magnificent potential of heavy rare earth elements for low-pressure stability. Here, we designed $XTmH_{12}$ (X = Y, Yb, Lu, and La) to obtain higher T_c while maintaining low pressure stability. Most prominently, $YbTmH_{12}$ can stabilize at a pressure of 60 GPa. Compared with binary TmH_6 hydride, its T_c was increased to 48 K. The results provide an effective method for the rational design of moderate pressure stabilized hydride superconductors.

Keywords Hydrides, High pressure, Superconductivity, First principles calculation

Since Kamerlingh Onnes discovered that mercury (Hg) suddenly starts carrying a current without resistance at an extremely low temperature in 1911[1,2], the achievement of room temperature superconductor is a dream for the superconductivity research. The theory that hydrogen can be metallized at high pressure was developed in 1935 and was proposed by Winger and Huntington[3]. According to the theory of superconductivity proposed by Bardeen, Cooper and Schrieffer in 1957, the transition temperature of superconductivity is proportional to the Debye temperature[4]. Due to this theory, hydrogen, the lightest element, would be the prospect of room-temperature superconductor after metallization[5], but because of the difficulty of the hydrogen metallization[6,7], the theory about hydrogen pre-compression was proposed by Ashcroft that the hydrogen-rich compounds could be a great option for the high T_c superconductors[8,9]. The theory of chemical pre-compression refers to the addition of other elements to the synthesized hydrogen-rich compounds at a lower pressure than synthesizing pure hydrogen[10]. Based on this conclusion, many great hydrogen-rich compounds have been designed and predicted to be potential superconductors with high T_c[11–13]. The first successful predictions were H_3S and LaH_{10} with high T_c exceeding 200 K[14–16], and these predictions were successfully confirmed by experiment soon[17–20].

Over these years, with the efforts of our researchers, almost all binary hydrides were explored, people commence the study of ternary hydride formed by adding a new element into binary hydrides. In 2019, Li_2MgH_{16} with the highest T_c to date (473 K at 250 GPa), designed by filling the anti-bonding orbital of the H_2 molecular unit of MgH_{16} with the element Li[21]. H–C–S compounds and Lu–N–H compounds have been widely studied for some time due to the claimed observation of room temperature superconductivity. However, there are still some controversial issues about the stoichiometry and the crystal structure[22–25]. Recently, a new kind of fluorite-type clathrate ternary hydrides AXH_8 (A = Ca, Sr, Y, La, X = B, Be, Al) in the main chain of hydrogen alloys has been predicted[26]. The most prominent, LaBeH8, is dynamically stable down to 20 GPa and has a high T_c up to 185 K. The exciting thing is that the cubic clathrate superhydrides $La_xY_{1-x}H_{6,10}$ have been experimentally synthesized by laser heating of yttrium-lanthanum alloys, which exhibited a maximum critical temperature T_c of 253 K without increasing pressure[27]. According this experiment, it is practicable to incorporate a metal element in the clathrate hydride to keep the compounds steadily.

It is a widespread attention about the prominent superconductivity of the clathrate hydrides. Clathrate hexahydrides *Im*-3 *m*-XH_6 (X = Mg, Ca, Sc, Y, La, Tm, Yb, Lu) are widespread in alkaline earth and rare earth metal superhydrides[16,28–32]. In this structure, there is a body-centered cube (bcc) with center occupied by a metal atom, and there is a H_{24} cage of hydrogen atoms in the void of the bcc lattice. CaH_6 and YH_6 have been experimentally synthesized with high T_cs of 215 K at 172 GPa[33,34] and 227 K at 166 GPa, respectively[35]. Theoretically predicted

[1]School of Physical Science and Technology, Institute of High Pressure Physics, Ningbo University, Ningbo 315211, People's Republic of China. [2]College of Physics, Jilin University, Changchun 130012, People's Republic of China. ✉email: dumingyang@nbu.edu.cn; cuitian@nbu.edu.cn

T_cs of MgH_6, ScH_6 and LaH_6 are 260 K at 300 GPa, 147 K at 285 GPa and174 K at 100 GPa, respectively. YbH_6 and LuH_6 in full *4f*.-orbital shells are predicted to exhibit high T_c superconductivity at relatively low pressures (145 K, 70 GPa vs. 273 K, 100 GPa, respectively)[32]. With unfilled *4f*. orbitals, TmH_6 is stable at 50 GPa, but has a relatively low T_c at 25 K. There was a report that the structures of superhydrides at low pressure could keep stable by *f* electrons, such as lanthanide clathrate hydrides CeH_9[36], PrH_9[37] and NdH_9[38]. Although the filling of the metal atoms' *f* orbital could make the structure more stable at low pressure, according to current research results, the T_cs of hydrides with unfilled *4f*. orbitals are mostly very low.

The properties of TmH_6, YbH_6 and LuH_6 indicated the magnificent potential of such structures for low-pressure stability. In alkaline earth and rare earth metals hydrides *Im*-3 *m*-XH_6 are common, such as CaH_6[28], MgH_6[29], YH_6[15,16,30], ScH_6[31], (Tm/Yb/Lu)H_6[32]. The structure can also be extended into the ternary structure *Pm*-3 *m*-ABH_{12}, such as (Y,Ca)H_6[39–41], (Mg,Ca)H_6[42], (Sc,Ca)H_6[43], (La,Y)H_6[44], (Ca/Sc/Y,Yb/Lu)H_6[45]. In recent years, based on this sodalite-like clathrate structure, we have designed a series of high-temperature superconductors that can be stable under moderate pressures by adding heavy rare earth elements Yb/Lu to sodalite-like clathrate hydrides[45]. Among them, Y_3LuH_{24} and YLu_3H_{24} are the room-temperature superconductors with the lowest stabilizing pressure predicted by current theory (283 K, 120 GPa and 288 K, 110 GPa, respectively). This result shows that room-temperature superconductivity of hydrogen-based superconductors is possible at medium pressure.

In this work, we designed $XTmH_{12}$ (X = Y, Yb, Lu, and La) to obtain higher T_c while maintaining low pressure stability. Most prominently, $YbTmH_{12}$ can stabilize at 60 GPa. Compared with binary TmH_6 hydride, its T_c was increased to 48 K. The results provide an effective method for the rational design of moderate pressure stabilized hydride superconductors.

Results

First, we designed a series of ternary clathrate hydrides $YTmH_{12}$ based on the sodalite-like clathrate structure $YLuH_{12}$[45]. The crystal structure of *Pm*-3 *m*-$YLuH_{12}$ is shown in Fig. 1. The atoms Y, Tm, and H occupy the 1*b* (0.5, 0.5, 0.5), 1*a* (0, 0, 0), and 12 h (0.25322, 0, 0) Wyckoff positions in the crystal structure. In this structure, there are a bcc lattice of metal atoms and a H_{24} cage which is formed by the hydrogen atom occupying all the tetrahedral void of the lattices, as shown in Fig. 1, and the H_{24} cage is formed by six H-square and eight H-hexagon rings, with two classes of unequal H atoms. In many alkaline earth metals and rare earth metal hydrides there are this kind of structure consisting of metal atom and H_{24} cage. There are two H_2 accepting electrons from the central metal atoms to form an H_4 unit, which serves as the cornerstone for the construction of a three-dimensional sodalite gabion and thus makes the structure stable. This unique structure partially occupies the degenerate orbit at the center of the region. The resulting dynamic Jahn–Teller effect contributes to enhanced electron–phonon coupling and leads to high T_c superconductivity.

As is well-known, the impact of the electron correlation effects is particularly significant for 4*f*. systems. In our previous work, we calculated the equation of state (EOS) for YbH_2 and compared it with the experimental EOS to assess the reliability of our DFT calculations[32]. One can see that there is a good agreement between the theory and experiment for the high-pressure phase $P6_3/mmc$ of YbH_2. The authors of previous work concerned with ytterbium hydrides[46], used a Hubbard U = 5 eV for lower pressure phases and U = 0 eV for high-pressure phases to reproduce available experimental data, in clear agreement with our results. Therefore, in this work, we select GGA and U = 0 eV for calculation of 4*f* systems.

Next, we try to extend $YTmH_{12}$ to more compounds. In the designed $XTmH_{12}$ structure, at least one of the "pre-compressor" metal atoms is heavy rare earth element Tm, and the other element has a similar radius with Tm, including Na, K, Mg, Ca, Sr, Sc, Y, Yb, Lu, La. Then we calculated the phonon dispersion for all possible components in the pressure range of 50–200 GPa. The stability of the replaced structure is reflected in Fig. 1, we determined that only Y, Yb, Lu and La can stabilize dynamically this ternary sodalite-like clathrate structure.

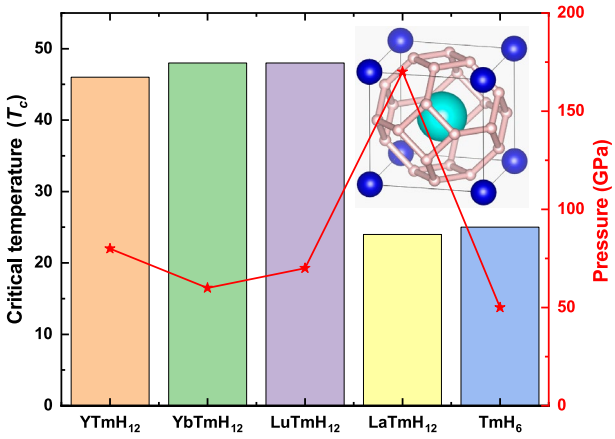

Figure 1. Crystal structures of *Pm*-3 *m*-$XTmH_{12}$ at 150 GPa, superconducting critical temperature T_c dynamically stability of compounds $XTmH_{12}$ (X = Y, Yb, Lu and La).

To determine the thermodynamic stability of these structures, we performed structure searches at a pressure of 100–200 GPa, focusing on $XTmH_{12}$ (X = Y, Yb, Lu and La) compositions with 1 to 2 formula units. As shown in Fig. 2, None of the structures *Pm*-3 *m*-$XTmH_{12}$ have the lowest enthalpy values, which means they are all metastable phases. The enthalpy of *Pm*-3 *m*-$YTmH_{12}$ and *Pm*-3 *m*-$LaTmH_{12}$ are higher than that of binary hydrides $YH_6 + TmH_6$ and $LaH_6 + TmH_6$, respectively. *Pm*-3 *m*-$YbTmH_{12}$ and *Pm*-3 *m*-$LuTmH_{12}$ are stable compared to the binaries $YbH_6 + TmH_6$ and $LuH_6 + TmH_6$, respectively, but their enthalpy are higher than that of the other ternary hydrides, such as *C*2/*c*-$YbTmH_{12}$ and *Fd*-3 *m*-$LuTmH_{12}$. This means that some difficulties need to be overcome in the experiment to synthesize these structures. However, metastable stable phases can also be synthesized experimentally and even dominate over thermodynamically stable phases[47,48].

We calculated their electronic band structures and projected density of states (PDOS). It can be clearly seen that the DOS value of the s electron of H near the Fermi surface is higher than that of the p and d electrons of the metal element. This is because H does not exist in molecular form, but forms a H_{24} cage. However, compared to other high-T_c hydrides with H_{24} cage, such as CaH_6, YH_6, and LuH_6, the DOS values of H's s electrons near the Fermi plane in these structures are not high enough, which is not good news for searching for high-temperature superconductors in hydrides. Furthermore, it is worth mentioning that the DOS of $XTmH_{12}$ has extremely high peaks near the Fermi surface. This is mainly due to the 4*f* orbitals from heavy rare earth elements form a set of localized and almost non-dispersive bands in $XTmH_{12}$. These bands will appear in different positions depending on the outermost electrons of the element. The bands from Tm atom with unfilled 4*f* orbitals appear at the Fermi level in $YTmH_{12}$ (see Fig. 3a), and the bands from Yb atom with full-filled 4*f* orbitals appear about 1 eV below the Fermi level (see Fig. 3b). The bands from Tm atom with unfilled 4*f* orbitals also appear at the Fermi level in $LaTmH_{12}$ (see Fig. 3c), this means that the species of the other metal element has almost no effect on the energy level at which the *4f* electron appears. The bands from Lu atom appear about 6 eV below the Fermi level (see Fig. 3d) because of full-filled 4*f* orbitals and an extra 5d electron. The *f* electrons can enhance the chemical compression effects from metallic elements, helping to stabilize the structure at lower pressures.

To make the prediction more reliable, evaluation of the impact of the electron correlation effects is desired. Therefore, we calculated the band structure using U = 5 eV to figure out how Hubbard-U may modify the band structure (see Fig. S1 in Supplementary Material). After considering U = 5 eV, one flat band is lifted up into the unoccupied regime. This means that the occupation of 4*f* states is changed, that could have substantial impact on the electron–phonon coupling physics. Future studies will focus on the impact of U to pairing strength.

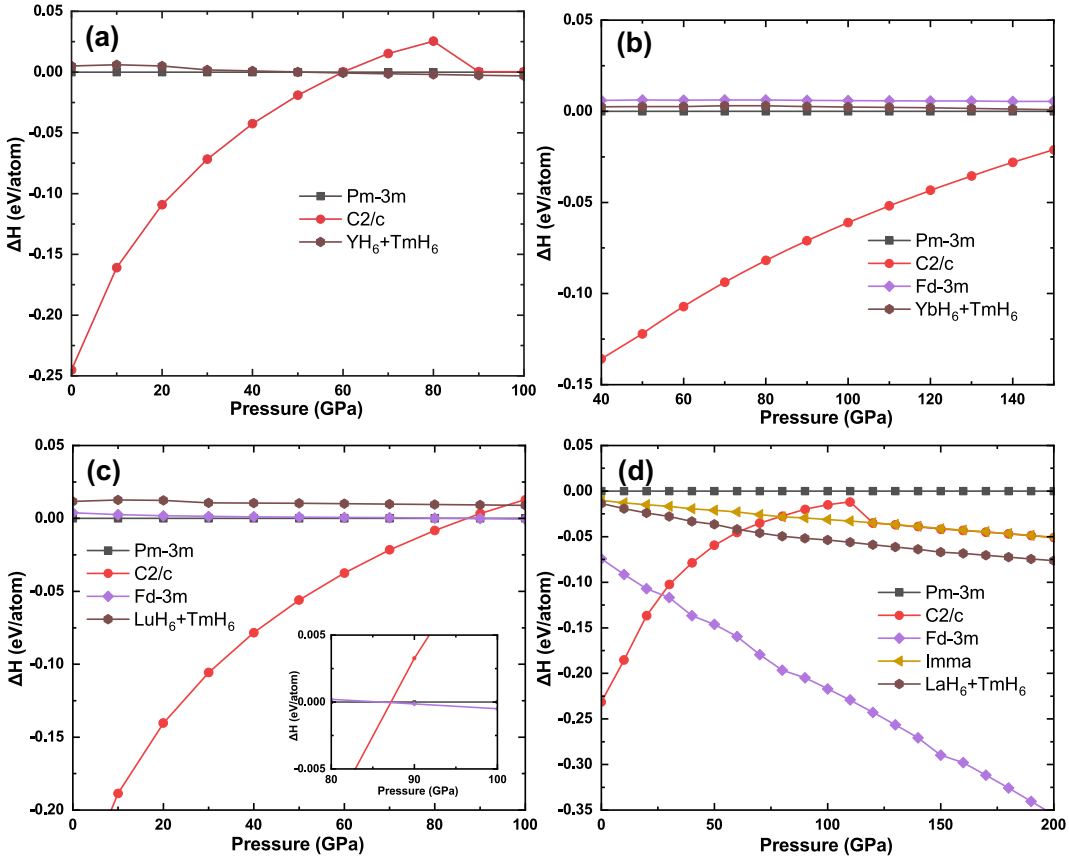

Figure 2. Calculated enthalpies per (**a**) $YTmH_{12}$, (**b**) $YbTmH_{12}$, (**c**) $LuTmH_{12}$, (**d**) $LaTmH_{12}$ as the function of pressure.

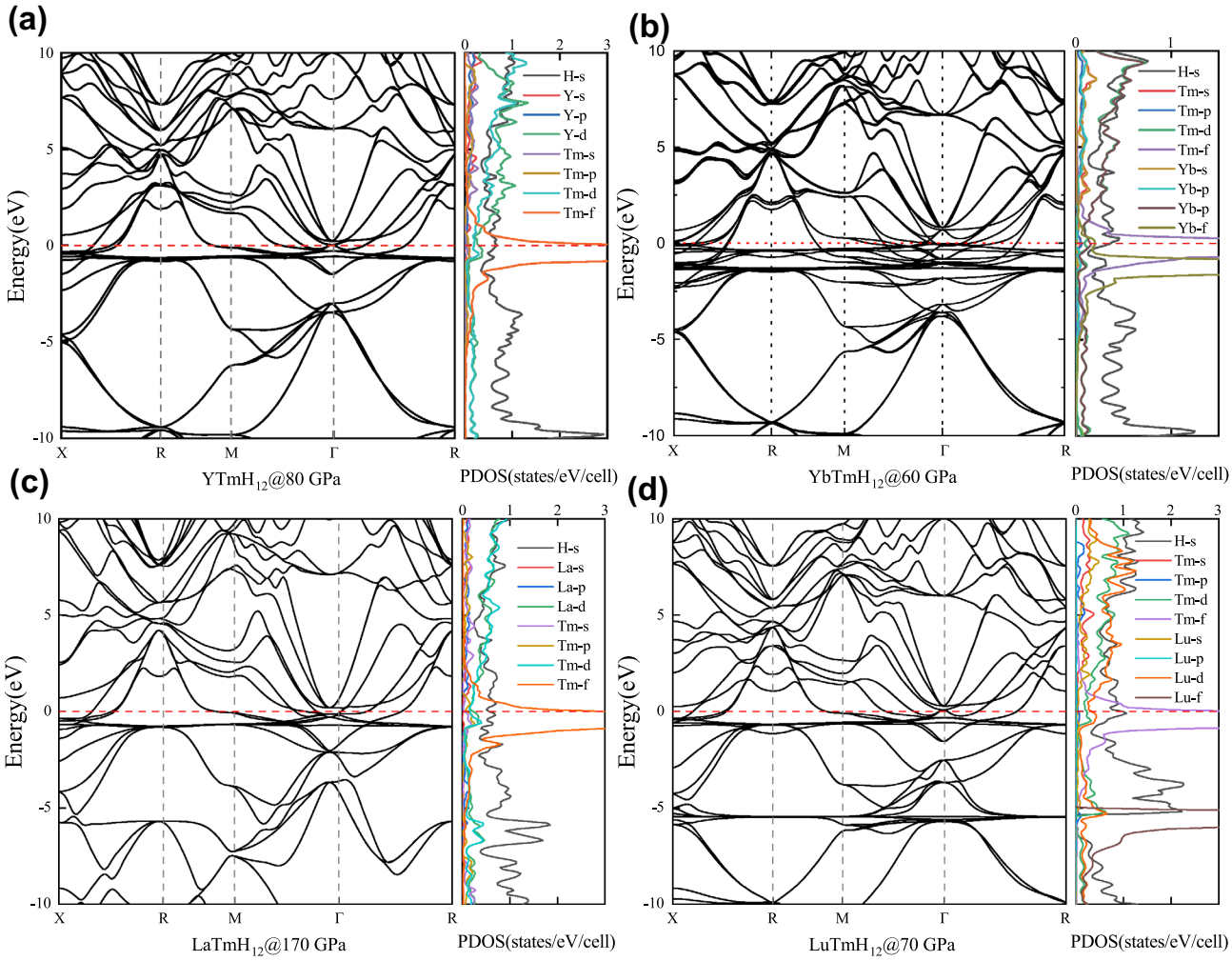

Figure 3. Calculated electronic band structures and projected density of states for (**a**) $YTmH_{12}$, (**b**) $YbTmH_{12}$, (**c**) $LuTmH_{12}$, (**d**) $LaTmH_{12}$.

Discussion

Then, we have compared the electronic density of states at the Fermi level (N_{Ef}) in $YTmH_{12}$, $YbTmH_{12}$, $LuTmH_{12}$ and $LaTmH_{12}$ and binary hexahydrides, including YH_6, TmH_6, YbH_6, LuH_6, LaH_6, as shown in Table 1. Benefit by *4f* electrons from heavy rare earth elements Tm, large electronic density of states at the Fermi level in the $XTmH_{12}$ is observed, much higher than that of the binary hexahydrides. The large H-derived electronic density

Compounds	Pressure (GPa)	λ	ω_{log} (K)	N_{Ef}	States/spin/Ry/cell					T_c (K)
					X-d	X-f	Tm-d	Tm-f	H–s	
$YTmH_{12}$	80	1.09	583	32.4	2.1	0	1.3	24.6	4.4	40–46
$YbTmH_{12}$	60	1.04	657	37.6	1.2	1.5	0.7	31.6	2.6	42–48
$LuTmH_{12}$	70	1.10	596	32.4	2.2	0	1.4	22.6	6.2	42–48
$LaTmH_{12}$	170	0.79	530	30.2	1.7	0	1.2	23.0	4.3	19–24
YH_6	120	3.06	829	4.7	2.0	0	–	–	2.2	251–264[30]
TmH_6	50	0.72	612	29.6	–	–	0.7	27.4	1.3	19–25[32]
YbH_6	70	2.22	652	8.4	1.0	4.3	–	–	2.7	121–131[32]
LuH_6	100	3.60	751	4.8	0.1	0	–	–	4.5	227–243[32]
LaH_6	100	1.83	1244	4.5	0.8	0	–	–	3.6	156–174[16]

Table 1. The calculated electron–phonon coupling (EPC) parameter λ, logarithmic average phonon frequency ω_{log}, electron density of states at the Fermi level (N_{Ef}, states/spin/Ry/cell), angular momentum components of the DOS at the Fermi level, superconducting critical temperature T_c for compounds $YTmH_{12}$, $YbTmH_{12}$, $LuTmH_{12}$ and $LaTmH_{12}$ and binary hexahydrides, including YH_6, TmH_6, YbH_6, LuH_6, LaH_6.

of states at the Fermi level is beneficial for strong electron–phonon coupling (EPC) parameter λ. Generally speaking, N_{Ef} indicates all of the candidate electrons to form Cooper pairs. It is clear that the large N_{Ef} plays a positive role in enhancing the EPC λ. However, from the aspect of partial DOS, the contribution from H to the electronic density of states at the Fermi level in $XTmH_{12}$ is not higher than the cases in binary hexahydrides. This suggests that the *4f* electrons will play no role in superconductivity. The contrasting EPC λ in these clathrate hexahydrides is mainly attributed to the disparate intensity of H electrons interacting with optic phonons, rather than the contributions from global electronic structures. Papaconstantopoulos et al. apply the Gaspari-Gyorffy theory to determine that, in CaH_6, the acoustic modes associated with Ca contribute only 7% to the total value of λ, in contrast to the optic modes associated with hydrogen which contribute 93% for the H[49]. And in LaH_{10}, La has only a 2% contribution[50].

The calculated T_cs by the Allen-Dynes modified McMillan equation[51] are shown in Table 1. $LaTmH_{12}$ has a T_c of 19–24 K at 170 GPa. This is not only much higher than the minimum stabilization pressure of 50 GPa for TmH_6, but also higher than the pressure of 100 GPa for LaH_6. $LaTmH_{12}$ requires higher pressures to remain stable, probably due to the excessive gap between the properties of La and Tm. This type of ternary clathrate structure requires the two metal elements to be close in radius and other properties to ensure H cage stability. Thus, $YTmH_{12}$ is able to stabilize at 80 GPa and exhibited T_c of 40–46 K. Both the minimum stabilization pressure and T_c are intermediate between the binary hydrides YH_6 and TmH_6. Yb and Lu, which are also heavy rare earth elements adjacent to Tm, have *f* electrons that can similarly enhance chemical pre-compression, so the stabilization pressure of their doped structures can be reduced even further, and $YbTmH_{12}$ and $LuTmH_{12}$ can be stabilized at 60 and 70 GPa, respectively, and exhibited T_c of 42–48 K. Their minimum stabilizing pressures and T_c also show a pattern intermediate to that of the binary hydrides.

Charge transfer has an important effect on the structure and properties of hydrides. Table 2 shows charges transferred for all thulium substituted clathrate hexahydrides. The *e* represents the total remaining electrons. Negative δ mean loss of electrons, positive δ mean gain of electrons. It can be seen that La is a very good electron donor and is able to provide sufficient electrons to the surrounding H. In $LaTmH_{12}$, each La atom can provide 2.25 electrons, ultimately making 0.21 electrons available for each H on average. However, the provision of sufficient electrons does not necessarily mean that superconductivity is favored, and may even create factors that are detrimental to superconductivity. In terms of charge transfer, the ability of Tm to provide electrons is stronger than that of Y and Yb, but unfortunately, the presence of *f* electrons severely constrains higher T_c in thulium substituted clathrate hexahydrides.

To determine the origin of the superconductivity in these superconductors, we calculated their phonon spectrum, projected phonon density of state (PHDOS), integral EPC parameter λ and Eliashberg spectral function $\alpha^2F(\omega)$. The superconductivity of superconductors comes mainly from strong electron–phonon coupling (EPC). So, we can look for the frequency range in which the EPC parameter λ grows rapidly, and vibration modes in this frequency range are the key to the superconductivity of this structure. As can be easily seen in Fig. 4, λ grows rapidly in two regions: the low-frequency region and the mid-frequency region. For example, in $LuTmH_{12}$, λ grows rapidly to 0.25 in the frequency range of 0–150 cm^{-1} and then grows slowly until the frequency range of 400–1000 cm^{-1}, where λ grows rapidly to 1.1, and then grows hardly at all (see Fig. 4a). In $YbTmH_{12}$, λ also grows rapidly in the frequency range of 500–1000 cm^{-1} (see Fig. 4b). By comparing the PHDOS of different elements, we can find the reason for the rapid growth of λ. The rapid growth of λ is mainly due to the vibrations of metal atoms in the low-frequency region (red and black peaks in PHDOS), while in the mid-frequency region it is due to the vibrations of hydrogen atoms (blue peaks in PHDOS). This corresponds to the two main sources of superconductivity in such clathrate hydrides: hydrogen on the hydrogen cage and the central metallic atom. In addition to this, it can be seen in Fig. 4c that the λ of $YTmH_{12}$ grows rapidly when the frequency is 300 cm^{-1}. On the phonon dispersion, there are soft phonon patterns near the R direction in this frequency range. This suggests that the softening of the optical branch of the phonon spectrum is also an important source of electron–phonon coupling. In $LuTmH_{12}$, λ grows rapidly to 0.25 in the frequency range of 0–150 cm^{-1} consistent with $YTmH_{12}$ (see Fig. 4d). However, in higher frequency range, λ grows much slower than that in $YTmH_{12}$, which leads to the low T_c in $LaTmH_{12}$.

In this work, we introduce other elements to improve the superconductivity of TmH_6, allowing the newly formed thulium substituted clathrate hexahydrides $XTmH_{12}$ (X = Y, Yb, Lu and La) to have the higher T_c while

Compounds	Pressure (GPa)	δ(X)	δ(Tm)	δ(H)
$YTmH_{12}$	80	−1.09	−1.19	0.19
$YbTmH_{12}$	60	−0.83	−1.09	0.16
$LuTmH_{12}$	70	0.94	−2.54	0.13
$LaTmH_{12}$	170	−2.25	−0.25	0.21
YH_6	120	−1.38	–	0.23
TmH_6	50	–	−0.91	0.15
YbH_6	70	−0.96	–	0.16
LuH_6	100	−0.66	–	0.11
LaH_6	100	−1.44	–	0.24

Table 2. Charges transferred for compounds (a) $YTmH_{12}$, (b) $YbTmH_{12}$, (c) $LuTmH_{12}$, (d) $LaTmH_{12}$. Negative δ mean loss of electrons, positive δ mean gain of electrons.

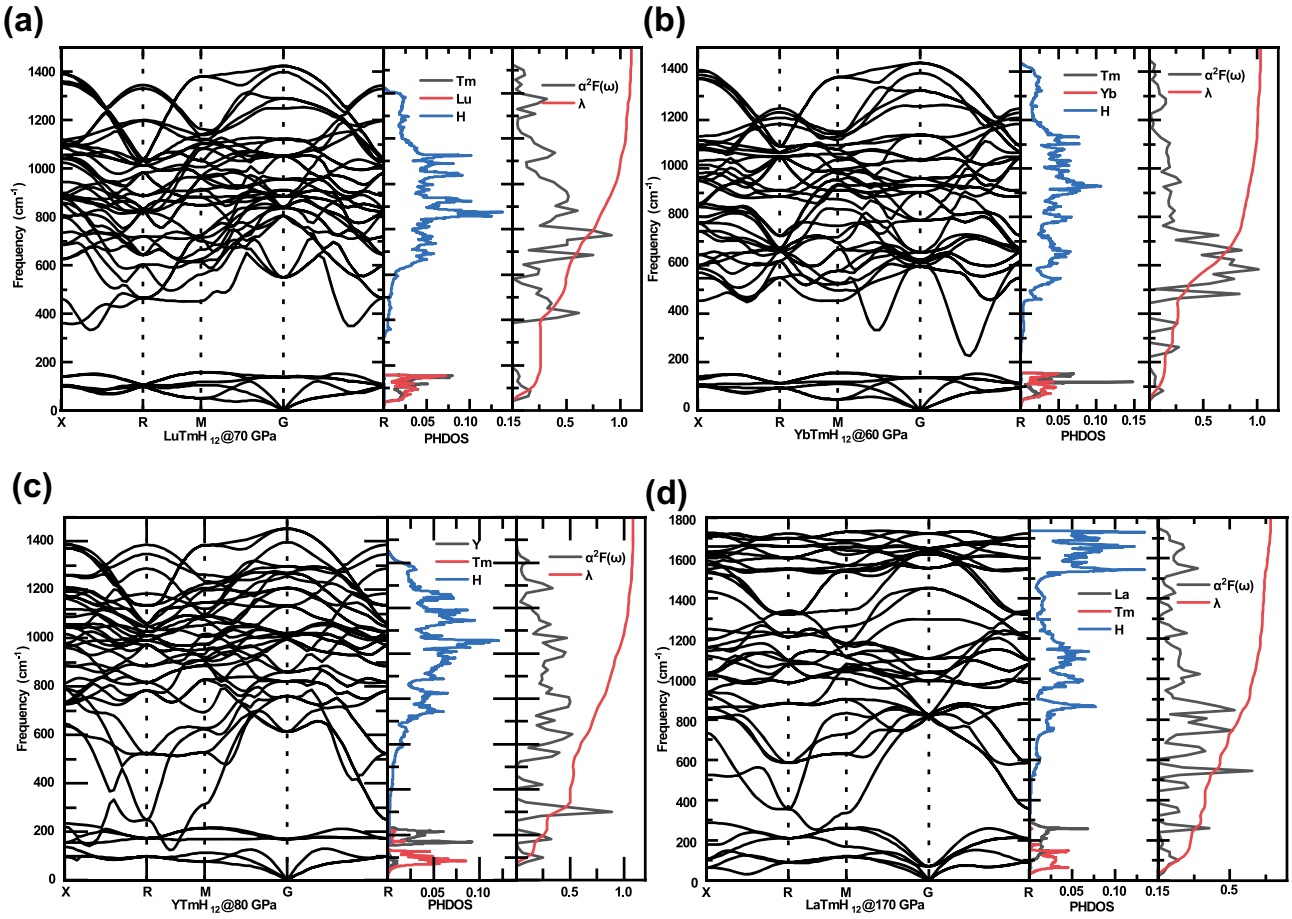

Figure 4. The calculated phonon band structure, PHDOS, electron–phonon coupling (EPC) parameter λ, and Eliashberg spectral function $\alpha^2F(\omega)$ of (**a**) $LuTmH_{12}$, (**b**) $YbTmH_{12}$, (**c**) $YTmH_{12}$, (**d**) $LaTmH_{12}$.

maintaining low-pressure stability. Most prominently, $YbTmH_{12}$ can be stabilized at a pressure of 60 GPa. Its T_c is elevated compared to the binary TmH_6, reaching 48 K. The results provide an effective method for the successful design of hydride superconductors at moderate pressures.

Computational methods

The candidate phases of $XTmH_{12}$ (X = Y, Yb, Lu, and La) are predicted using the ab initio Random Structure search (AIRSS) technique[52,53]. The selected cut-off energy of the projected augmented wave (PAW)[54] is 400 eV. The sampling density of the Brillouin district is $2\pi \times 0.07$ Å^{-1}.The ultra-soft potentials is dynamically generated by the method of pseudo-potentials. The valence electrons in the electronic states of Y, Tm, Yb, Lu and La atoms are $4s^24p^65s^24d^1$, $4f^{13}5s^25p^66s^2$, $4f^{14}5s^25p^66s^2$, $4f^{14}5p^65d^16s^2$, $5s^25p^65d^16s^2$, respectively.

Structural relaxation, calculations of enthalpies, band structures, density of states and charge transfer of $XTmH_{12}$ (X = Y, Yb, Lu and La) at different pressures were calculated by the Cambridge Serial Total Energy Package (CASTEP)[55]. We use the generalized gradient approximation (GGA)[56] with the Perdew-Burke-Ernzerh of (PBE) parametrization[57] as the exchange–correlation function. For the plane wave, we chose a cut-off energy of 800 eV. The sampling density of the Brillouin region is $2\pi \times 0.03$ Å^{-1}. The pseudo-potential is dynamically generated by the ultra-soft potential.

Phonon dispersion, electron–phonon coupling and Eliashberg spectral function $\alpha^2F(\omega)$ of $XTmH_{12}$ (X = Y, Yb, Lu and La) were calculated by the Quantum-ESPRESSO (Open-Source Package for Research in Electronic Structure, Simulation, and Optimization)[58]. With an ultra-soft potential and a cut off energy of 90 Ry, all $XTmH_{12}$ (X = Y, Yb, Lu, La) in the first Brillouin region have a k-point grid of $12 \times 12 \times 12$ and a q-point grid of $4 \times 4 \times 4$, respectively. The superconducting transition temperatures of $XTmH_{12}$ (X = Y, Yb, Lu and La) are estimated through the Allen–Dynes-modified McMillan equation (A-D-M) with correction factors[51,59]:

$$T_c = \frac{f_1 f_2 \omega_{log}}{1.2} exp\left[-\frac{1.04(1+\lambda)}{\lambda - \mu^*(1+0.62\lambda)}\right]$$

λ and ω_{log} are given by:

$\lambda = 2\int_0^\infty \frac{\alpha^2F(\omega)}{\omega} d\omega$ and $\omega_{log} = exp\left(\frac{2}{\lambda}\int_0^\infty \frac{d\omega}{\omega}\alpha^2F(\omega)ln\omega\right)$

f_1 and f_2 are given by:

$$f_1 = \sqrt[3]{\left[1 + \left(\frac{\lambda}{2.46(1+3.8\mu^*)}\right)^{\frac{3}{2}}\right]} \text{ and } f_2 = 1 + \frac{\left(\frac{\omega_2}{\omega_{log}} - 1\right)\lambda^2}{\lambda^2 + \left[1.82(1+6.3\mu^*)\frac{\overline{\omega}_2}{\omega_{log}}\right]}$$

average frequencies $\overline{\omega}_2$ is given by:

$$\overline{\omega}_2 = \sqrt{\frac{2}{\lambda}} \int_0^\infty \frac{d\omega}{\omega} \alpha^2 F(\omega) \omega d\omega$$

The typical value of Coulomb pseudo-potential μ* was set as 0.1–0.13.

Received: 22 January 2024; Accepted: 6 May 2024
Published online: 10 May 2024

References

1. Liu, T. *et al.* Shockwave-loading-induced enhancement of Tc in superconducting $Bi_2Sr_2CaCu_2O_8$+δ. *Sci. Rep.* **7**, 6710. https://doi.org/10.1038/s41598-017-06887-5 (2017).
2. Deng, L. *et al.* Pressure-induced high-temperature superconductivity retained without pressure in FeSe single crystals. *Proc. Natl. Acad. Sci. USA* **118**, e2108938118. https://doi.org/10.1073/pnas.2108938118 (2021).
3. Wigner, E. & Huntington, H. B. On the possibility of a metallic modification of hydrogen. *J. Chem. Phys.* **3**, 764–770. https://doi.org/10.1063/1.1749590 (1935).
4. Bardeen, J., Cooper, L. N. & Schrieffer, J. R. Microscopic theory of superconductivity. *Phys. Rev.* **106**, 162–164. https://doi.org/10.1103/PhysRev.106.162 (1957).
5. Ashcroft, N. W. Metallic hydrogen: A high-temperature superconductor?. *Phys. Rev. Lett.* **21**, 1748. https://doi.org/10.1103/PhysRevLett.21.1748 (1968).
6. Dias, R. P. & Silvera, I. F. Observation of the Wigner-Huntington transition to metallic hydrogen. *Science* **355**, 715–718. https://doi.org/10.1126/science.aal1579 (2017).
7. Loubeyre, P., Occelli, F. & Dumas, P. Synchrotron infrared spectroscopic evidence of the probable transition to metal hydrogen. *Nature* **577**, 631. https://doi.org/10.1038/s41586-019-1927-3 (2020).
8. Quan, Y., Ghosh, S. S. & Pickett, W. E. Compressed hydrides as metallic hydrogen superconductors. *Phys. Rev. B* **100**, 184505. https://doi.org/10.1103/PhysRevB.100.184505 (2019).
9. Chen, X.-J. Exploring high-temperature superconductivity in hard matter close to structural instability. *Matter. Radiat. Extremes* **5**, 068102. https://doi.org/10.1063/5.0033143 (2020).
10. Ashcroft, N. W. Hydrogen dominant metallic alloys: High temperature superconductors?. *Phys. Rev. Lett.* **92**, 4. https://doi.org/10.1103/PhysRevLett.92.187002 (2004).
11. Du, M., Zhao, W., Cui, T. & Duan, D. Compressed superhydrides: the road to room temperature superconductivity. *J. Phys. Condens. Matter* **34**, 173001 (2022).
12. Duan, D. F. *et al.* Structure and superconductivity of hydrides at high pressures. *Natl. Sci. Rev.* **4**, 121–135. https://doi.org/10.1093/nsr/nww029 (2017).
13. Gor'kov, L. P. & Kresin, V. Z. Colloquium: High pressure and road to room temperature superconductivity. *Rev. Mod. Phys.* **90**, 16. https://doi.org/10.1103/RevModPhys.90.011001 (2018).
14. Duan, D. F. *et al.* Pressure-induced metallization of dense (H2S)(2)H-2 with high-T-c superconductivity. *Sci. Rep.* **4**, 6. https://doi.org/10.1038/srep06968 (2014).
15. Liu, H. Y., Naumov, I., Hoffmann, R., Ashcroft, N. W. & Hemley, R. J. Potential high-T-c superconducting lanthanum and yttrium hydrides at high pressure. *Proc. Natl. Acad. Sci. USA* **114**, 6990–6995. https://doi.org/10.1073/pnas.1704505114 (2017).
16. Peng, F. *et al.* Hydrogen clathrate structures in rare earth hydrides at high pressures: possible route to room-temperature superconductivity. *Phys. Rev. Lett.* **119**, 6. https://doi.org/10.1103/PhysRevLett.119.107001 (2017).
17. Drozdov, A. P., Eremets, M. I., Troyan, I. A., Ksenofontov, V. & Shylin, S. I. Conventional superconductivity at 203 kelvin at high pressures in the sulfur hydride system. *Nature* **525**, 73. https://doi.org/10.1038/nature14964 (2015).
18. Einaga, M. *et al.* Crystal structure of the superconducting phase of sulfur hydride. *Nat. Phys.* **12**, 835–838. https://doi.org/10.1038/nphys3760 (2016).
19. Drozdov, A. P. *et al.* Superconductivity at 250 K in lanthanum hydride under high pressures. *Nature* **569**, 528. https://doi.org/10.1038/s41586-019-1201-8 (2019).
20. Somayazulu, M. *et al.* Evidence for superconductivity above 260 K in Lanthanum superhydride at megabar pressures. *Phys. Rev. Lett.* **122**, 6. https://doi.org/10.1103/PhysRevLett.122.027001 (2019).
21. Sun, Y., Lv, J., Xe, Y., Lu, H. Y. & Ma, Y. M. Route to a superconducting phase above room temperature in electron-doped hydride compounds under high pressure. *Phys. Rev. Lett.* **123**, 5. https://doi.org/10.1103/PhysRevLett.123.097001 (2019).
22. Wang, T. *et al.* Absence of conventional room-temperature superconductivity at high pressure in carbon-doped H3S. *Phys. Rev. B* **104**, 064510. https://doi.org/10.1103/PhysRevB.104.064510 (2021).
23. Gubler, M., Flores-Livas, J. A., Kozhevnikov, A. & Goedecker, S. Missing theoretical evidence for conventional room-temperature superconductivity in low-enthalpy structures of carbonaceous sulfur hydrides. *Phys. Rev. Mater.* **6**, 014801. https://doi.org/10.1103/PhysRevMaterials.6.014801 (2022).
24. Du, M., Zhang, Z., Cui, T. & Duan, D. Pressure-induced superconducting CS2H10 with an H3S framework. *Phys. Chem. Chem. Phys.* **23**, 22779. https://doi.org/10.1039/D1CP03270D (2021).
25. Huo, Z. *et al.* First-principles study on the conventional superconductivity of N-doped fcc-LuH_3. *Matter. Radiat. Extremes* **8**, 038402. https://doi.org/10.1063/5.0151844 (2023).
26. Zhang, Z. *et al.* Design principles for high-temperature superconductors with a hydrogen-based alloy backbone at moderate pressure. *Phys. Rev. Lett.* **128**, 047001. https://doi.org/10.1103/PhysRevLett.128.047001 (2022).
27 Semenok, D. V. *et al.* Superconductivity at 253 K in lanthanum–yttrium ternary hydrides. *Mater. Today* **48**, 18–28. https://doi.org/10.1016/j.mattod.2021.03.025 (2021).
28. Wang, H., Tse, J. S., Tanaka, K., Iitaka, T. & Ma, Y. Superconductive sodalite-like clathrate calcium hydride at high pressures. *Proc. Natl. Acad. Sci. USA* **109**, 6463. https://doi.org/10.1073/pnas.1118168109 (2012).
29. Feng, X., Zhang, J., Gao, G., Liu, H. & Wang, H. Compressed sodalite-like MgH6 as a potential high-temperature superconductor. *RSC Adv.* **5**, 59292–59296. https://doi.org/10.1039/C5RA11459D (2015).
30. Li, Y. *et al.* Pressure-stabilized superconductive yttrium hydrides. *Sci. Rep.* **5**, 9948. https://doi.org/10.1038/srep09948 (2015).
31. Abe, K. Hydrogen-rich scandium compounds at high pressures. *Phys. Rev. B* **96**, 144108. https://doi.org/10.1103/PhysRevB.96.144108 (2017).

32 Song, H. *et al.* High Tc superconductivity in heavy rare earth hydrides. *Chin. Phys. Lett.* **38**, 107401. https://doi.org/10.1088/0256-307x/38/10/107401 (2021).
33. Ma, L. *et al.* High-temperature superconducting phase in clathrate calcium hydride CaH6 up to 215 K at a pressure of 172 GPa. *Phys. Rev. Lett.* **128**, 167001. https://doi.org/10.1103/PhysRevLett.128.167001 (2022).
34. Li, Z. *et al.* Superconductivity above 200 K discovered in superhydrides of calcium. *Nat. Commun.* **13**, 2863. https://doi.org/10.1038/s41467-022-30454-w (2022).
35 Troyan, I. A. *et al.* Anomalous high-temperature superconductivity in YH6. *Adv. Mater.* **33**, 2006832. https://doi.org/10.1002/adma.202006832 (2021).
36. Chen, W. *et al.* High-temperature superconducting phases in cerium superhydride with a Tc up to 115 K below a pressure of 1 megabar. *Phys. Rev. Lett.* **127**, 117001. https://doi.org/10.1103/PhysRevLett.127.117001 (2021).
37. Zhou, D. *et al.* Superconducting praseodymium superhydrides. *Sci. Adv.* **6**, 6849. https://doi.org/10.1126/sciadv.aax6849 (2020).
38. Zhou, D. *et al.* High-pressure synthesis of magnetic neodymium polyhydrides. *J. Am. Chem. Soc.* **142**, 2803–2811. https://doi.org/10.1021/jacs.9b10439 (2020).
39. Xie, H. *et al.* High-temperature superconductivity in ternary clathrate $YCaH_{12}$ under high pressures. *J. Phys. Condes. Matter.* **31**, 7. https://doi.org/10.1088/1361-648X/ab09b4 (2019).
40. Liang, X. *et al.* Potential high-Tc superconductivity in $CaYH_{12}$ under pressure. *Phys. Rev. B* **99**, 100505. https://doi.org/10.1103/PhysRevB.99.100505 (2019).
41. Zhao, W. *et al.* Pressure-induced high-Tc superconductivity in the ternary clathrate system Y-Ca-H. *Phys. Rev. B* **106**, 014521. https://doi.org/10.1103/PhysRevB.106.014521 (2022).
42 Sukmas, W., Tsuppayakorn-aek, P., Pinsook, U. & Bovornratanaraks, T. Near-room-temperature superconductivity of Mg/Ca substituted metal hexahydride under pressure. *J. Alloy. Compd.* **849**, 156434. https://doi.org/10.1016/j.jallcom.2020.156434 (2020).
43 Shi, L.-T. *et al.* Prediction of pressure-induced superconductivity in the novel ternary system ScCaH2n (n = 1–6). *J. Mater. Chem. C* **9**, 7284–7291. https://doi.org/10.1039/D1TC00634G (2021).
44. Song, P. *et al.* High-Tc superconducting hydrides formed by LaH24 and YH24 cage structures as basic blocks. *Chem. Matter.* **33**, 9501–9507. https://doi.org/10.1021/acs.chemmater.1c02371 (2021).
45. Du, M., Song, H., Zhang, Z., Duan, D. & Cui, T. Room-temperature superconductivity in Yb/Lu substituted clathrate hexahydrides under moderate pressure. *Research* **2022**, 9784309 (2022).
46. Klotz, S., Casula, M., Komatsu, K., Machida, S. & Hattori, T. High-pressure structure and electronic properties of YbD_2 to 34 GPa. *Phys. Rev. B* **100**, 020101. https://doi.org/10.1103/PhysRevB.100.020101 (2019).
47. Flores-Livas, J. A. *et al.* Interplay between structure and superconductivity: Metastable phases of phosphorus under pressure. *Phys. Rev. Mater.* **1**, 024802. https://doi.org/10.1103/PhysRevMaterials.1.024802 (2017).
48 Sun, W. *et al.* The thermodynamic scale of inorganic crystalline metastability. *Sci. Adv.* **2**, e1600225. https://doi.org/10.1126/sciadv.1600225 (2016).
49. Papaconstantopoulos, D. A., Mehl, M. J. & Economou, E. N. High-temperature superconductivity in the Ca-Sc-H system. *Phys. Rev. B* **108**, 224508. https://doi.org/10.1103/PhysRevB.108.224508 (2023).
50. Papaconstantopoulos, D. A., Mehl, M. J. & Chang, P. H. High-temperature superconductivity in LaH10. *Phys. Rev. B* **101**, 060506. https://doi.org/10.1103/PhysRevB.101.060506 (2020).
51. Allen, P. B. & Dynes, R. C. Transition temperature of strong-coupled superconductors reanalyzed. *Phys. Rev. B* **12**, 905–922. https://doi.org/10.1103/PhysRevB.12.905 (1975).
52. Pickard, C. J. & Needs, R. J. High-pressure phases of silane. *Phys. Rev. Lett.* **97**, 4. https://doi.org/10.1103/PhysRevLett.97.045504 (2006).
53. Pickard, C. J. & Needs, R. J. Ab initio random structure searching. *J. Phys. Condes. Matter.* **23**, 23. https://doi.org/10.1088/0953-8984/23/5/053201 (2011).
54. Kresse, G. & Joubert, D. From ultrasoft pseudopotentials to the projector augmented-wave method. *Phys. Rev. B* **59**, 1758–1775. https://doi.org/10.1103/PhysRevB.59.1758 (1999).
55. Clark, S. J. *et al.* First principles methods using CASTEP. *Z. Kristall.* **220**, 567–570. https://doi.org/10.1524/zkri.220.5.567.65075 (2005).
56. Ceperley, D. M. & Alder, B. Ground state of the electron gas by a stochastic method. *Phys. Rev. Lett.* **45**, 566 (1980).
57. Perdew, J. P., Burke, K. & Ernzerhof, M. Generalized gradient approximation made simple. *Phys. Rev. Lett.* **77**, 3865 (1996).
58. Giannozzi, P. *et al.* QUANTUM ESPRESSO: A modular and open-source software project for quantum simulations of materials. *J. Phys.-Condes. Matter.* **21**, 19. https://doi.org/10.1088/0953-8984/21/39/395502 (2009).
59. McMillan, W. L. Transition temperature of strong-coupled superconductors. *Phys. Rev.* **167**, 331 (1968).

Acknowledgements

This work was supported by the National Natural Science Foundation of China (Grants No. 52072188, No. 12122405 and No. 12274169), Program for Science and Technology Innovation Team in Zhejiang (Grant No. 2021R01004), Jilin Provincial Science and Technology Development Project (20210509038RQ), Natural Science Foundation of Zhejiang Province (Grants No. LQ24A040001) and the Fundamental Research Funds for the Provincial Universities of Zhejiang (SJLY2023003).

Author contributions

T.C. initiated the project. M.D. and H.H. performed the most of the theoretical calculations and contributed to the data interpretation and writing the manuscript. C.D. and H.S. contributed to the theoretical calculations. All authors contributed to the discussion and the final version of the manuscript.

Competing interests

The authors declare no competing interests.

Additional information

Supplementary Information The online version contains supplementary material available at https://doi.org/10.1038/s41598-024-61400-z.

Correspondence and requests for materials should be addressed to M.D. or T.C.